

TRAIL FOLLOWING OF TURBULENT WAKE USING ARTIFICIAL LATERAL LINE

Yingchen Yang¹, Saunvit Pandya¹, Craig Tucker¹, Douglas Jones²,
Jonathon Engel¹, Nannan Chen¹, Chang Liu¹

¹Micro and Nanotechnology Laboratory & ²Coordinated Science Laboratory
University of Illinois at Urbana-Champaign
Urbana, IL 61801, USA

ABSTRACT

Inspired by the unique flow imaging capability of fish lateral lines, we configured an artificial lateral line (ALL) in fish contour, and conducted biomimetic study on trail following of a hydrodynamic wake. The ALL consisted of 13 hot-film anemometers, and was integrated with a 3-degree of freedom robotic arm for movement in a 2-D plane. A circular cylinder was exposed in a water channel to generate the wake. Trail-following algorithm was developed based on wake characterization both numerically and experimentally, and was further optimized through applications of the ALL. We demonstrate that the robotic ALL can follow a wake successfully in various scenarios. Such efforts will lead to safer autonomous navigation of underwater vehicles in complex aquatic environment.

1. INTRODUCTION

A lateral line is a fluid sensory system ubiquitous in fish (Dijkgraaf, 1962). It contributes to rich behaviors and is essential to survival. A lateral line consists of spatially distributed neuromasts (Figure 1a), which are further categorized into superficial neuromasts (Figure 1b) and canal neuromasts (Figure 1c). Superficial neuromasts were described as detectors of the velocity of fluid, where as canal neuromasts rather detect the surrounding fluid's acceleration (Coombs and Janssen, 1990; Engelmann et al., 2000). Joint functioning of them enables a lateral line on spatial-temporal imaging of local hydrodynamic events, thus assists a diversity of tasks such as tracking prey and evading predator (Bleckmann, 1994), schooling (Partridge and Pitcher, 1980), and avoiding obstacles (Hassan, 1986). Of special interest to the present biomimetic research, Pohlmann et al. (2001) demonstrated that a nocturnal catfish could locate a piscine prey by accurately tracking its three-dimensional swim path from distance away in the absence of visible light. Liao et al. (2003) showed that a fish rode vortex motion in a cylinder wake for energy saving, enabled by the superb flow imaging capability of its lateral line.

To learn from fish lateral lines for engineering applications is of great importance. For example, equipped with an artificial lateral line, an autonomous underwater

vehicle (AUV) might be able to explore a complex aquatic environment freely and safely, even without vision and sonar assistances. This will be especially important when the AUV is in a dark or murky environment, or in a sonar blind zone. Another example, a most common reason for submarine accidents is collision, between two submarines, or one with a surface vehicle or a sea mountain. By imitating fish behavior on obstacle avoidance, a well-developed artificial lateral line on the hull of a submarine can surely diminish such tragedies. Being inspired by fish lateral lines, a well developed ALL can, in turn, facilitate fundamental studies of biological systems as well.

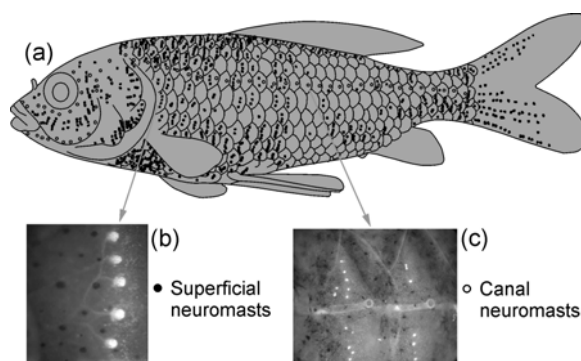


Figure 1: (a) Lateral line periphery. (b) Superficial neuromasts. (c) Canal neuromasts.

In the past a few years efforts have been made in our research group on development of such ALLs. Chen and Liu (2003) presented the first successful prototype of ALL, which was a MEMS-based hot-wire anemometer array on a silicon wafer. With assistance of specially developed algorithm by Pandya et al. (2006), Yang et al. (2006) demonstrated that the ALL was able to accurately localize an underwater vibration source, and detect a hydrodynamic trail. Most recently, Chen et al. (2007) showed a next-generation ALL based on biomimetic hair-cell sensors, and Yang et al. (2007) applied it to biologically relevant flow measurements. Yet, for all these ALLs, individual flow

sensors are spatially distributed in a linear format, and behavioral functionalities of ALLs were examined only in static conditions, namely, localization of a dipole source and detection of a wake.

While more sophisticated ALLs are underway via microfabrication techniques and sensor advancements, dynamic behaviors of an ALL are examined in parallel. In this paper we report our progress on trail following of a turbulent wake. To gain the flexibility on shape configuration of an ALL, conventional hot-film anemometers (HFAs) were employed to construct a hydrodynamically transparent robotic fish for development of trail-following techniques.

2. EXPERIMENTAL SETUP

Figure 2a shows the experimental setup. A bench-top water channel (ELD Inc., model 501) is used to create a steady current. A circular cylinder of $D = 12.7\text{mm}$ (diameter) is vertically fixed in the test section to generate a turbulent wake. The ALL is maneuvered by a computer controlled 3-degree-of-freedom stage system (Newport, models IMS600PP, IMS300PP, URS100PP). Thirteen HFAs (Dantec, model 55R11) are employed to construct the ALL; they are evenly distributed along a fish-like contour, as shown in details in Figure 2b. The contour is actually a NACA0015 airfoil of chord length 76.2mm, and the configured ALL is capable of rotating along an axis perpendicular to the airfoil at 40% of the chord length from the tip. While exposed in a wake, the ALL collects wake information from individual HFAs simultaneously. Via LabView interface the computer processes information, makes decision, and commands the motorized stage system to bring the ALL to the next position. Iteration of this procedure makes the ALL follow the wake, if decisions made from step to step are right.

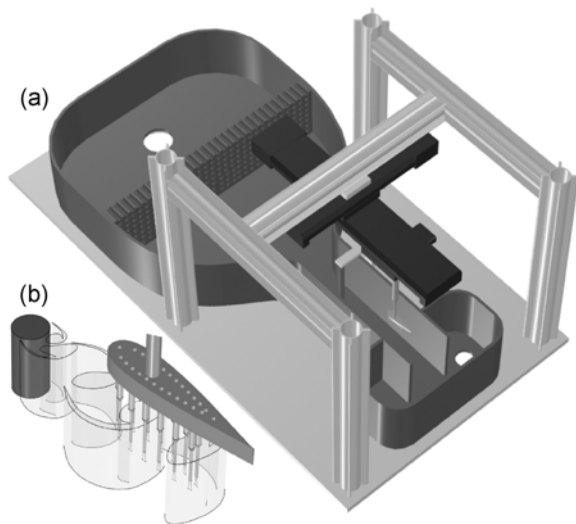


Figure 2: (a) Schematic showing experimental setup of wake following. (b) Close-up of ALL exposed in a cylinder wake.

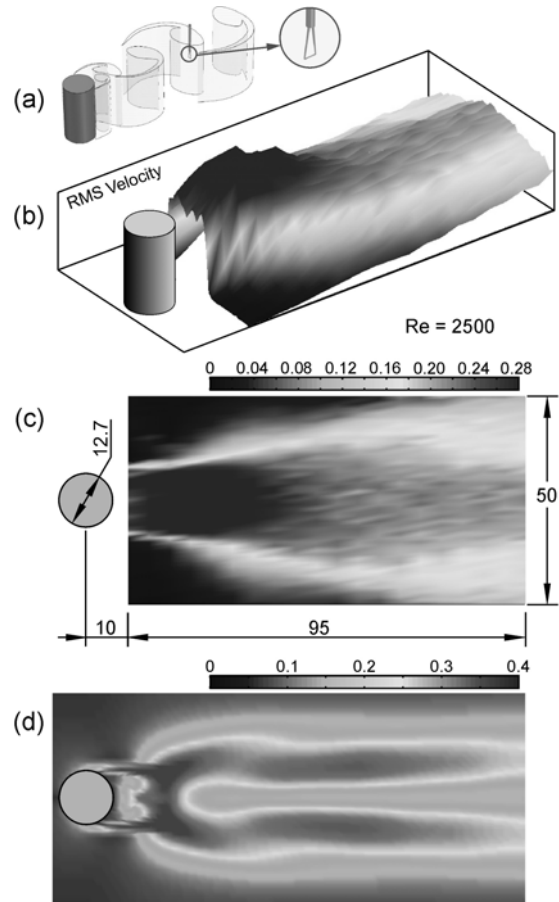


Figure 3: (a) Experimental setup for wake measurements. (b) Isotropic view of RMS velocity distribution, from experiments. (c) Plan view of RMS velocity distribution, from experiments. (d) Plan view of RMS velocity distribution, from CFD. All RMS velocities are normalized by inflow velocity.

3. ALGORITHM DEVELOPMENT

Algorithms play an essential role in decision-making. Preliminary investigation indicates that a simple but effective measure – RMS of the AC component of fluctuating velocities can serve this purpose well, especially when the wake is complex and characteristic frequencies are hard to identify. For algorithm development, the signature of a cylinder wake is first characterized by means of numerical simulation and experiments. In both cases Reynolds number of $Re = 2500$ is employed, which reflects the real flow condition for trail following. Numerically, a two-dimensional approach is made by counting in the sidewall effect of the water channel. Experimentally, a HFA is used to measure the wake point-by-point in a near wake region, as illustrated in Figures 3a and 3c. The corresponding RMS distribution of velocity fluctuation on a plane 4D below the free surface is presented in isotropic view and plan view in Figures 3b and 3c, respectively. Note that a single-wire HFA, which is employed in the present investigation, is not polarity sensitive to flow directions (Yang et al., 2007). For present setup, it measures the total vectorial velocity but yields scalar voltage output. For

direct comparison, total velocity from numerical simulation is resulted and treated as a scalar parameter, and the RMS distribution of its AC component is presented in plan view of Figure 3d. It is evident that experimental results differ from numerical ones dramatically. For RMS distributions along the wake, the experimental one is mountain-like with a flat peak across the wake, whereas the numerical one is valley-like with two sharp peaks alongside. The reasons for the difference are twofold. Numerically a two-dimensional simulation is performed to a three-dimensional wake; the three-dimensionality of the wake is further intensified by free surface interaction. Experimentally the measurement results are affected by the signal rectification, an intrinsic nature of HFAs (Yang et al., 2007). The originally developed algorithm based on numerical results is then adjusted to fit experimental measurements.

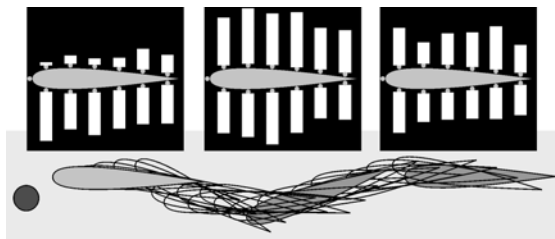


Figure 4: A tracking path with inserts showing signal distribution of the ALL at three typical instants.

Figure 4 shows a trail-following path of the ALL by applying such an algorithm. As illustrated in each step of Figure 4, the decision-making in each step is based on comparison of overall signal intensity from six HFAs on one side of the ALL with that of another six HFAs on the other side. The ALL always turns to the side with high signal intensity. Specifically, a large difference leads to a large rotation and a small translation, whereas a small difference yields a small rotation and a large translation. By evaluating the ratio of signal intensities on both sides, and by defining a threshold value of the ratio, stepwise movement of the ALL within specified limits of translation and rotation can be determined. To ensure the ALL moving towards the cylinder instead of running away, phase information, extracted via cross-correlation of adjacent HFAs, is also encoded into the algorithm. A wake following process is terminated through human interference based on observation.

4. TRAIL FOLLOWING

To justify the algorithm developed, and to optimize trail-following scheme, various experiments have been carried out under the same flow conditions. A cylinder of 12.7mm in diameter is vertically exposed in an inflow of velocity $U = 0.2\text{m/s}$ ($Re = 2500$), creating a wake behind it at vortex shedding frequency of 2.3Hz.

Figures 5a through 5c demonstrate three trail-following runs with different initial approaching angles. For each step of the following, data acquisition (DAQ) is done in 0.5s at a sample rate of 2048 samples/s, covering a little more than

one period of dominant velocity fluctuation induced by vortex shedding. Both DAQ and decision-making are performed while the ALL holds its position relative to the stationary cylinder. The translation may vary between 1mm and 5mm, and rotation between 3° and 10° , depending on the signal intensity ratio. It is evident that in all three runs the ALL has successfully followed the wake and reached the cylinder. However, repetitive experiments indicate that when the initial angle is greater than 40° , probability of failure increases, although below 40° a 100% success has been achieved. Another issue is that, for all the runs, the ALL hesitates too much by frequently adjusting its angular positions instead of moving forward quickly. This is partly due to the dynamic nature of the wake, and can be improved by increasing DAQ time. Figure 5d shows such improvement. Obviously an increase of DAQ time from 0.5s (Figure 5a) to 3s (Figure 5d) has made the tracking path smoother. Nonetheless, the overall trail-following time has been remarkably lengthened.

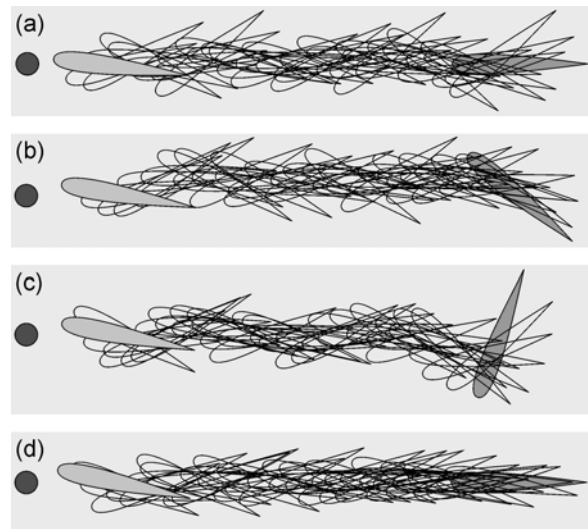


Figure 5: Step-by-step tracking paths. Stepwise motion control parameters: translation range 1mm to 5mm, rotation range 3° to 10° , speed limits 1mm/s in displacement and $1^\circ/\text{s}$ angularly, accelerations to start and stop each step $1\text{mm}/\text{s}^2$ in displacement and $1^\circ/\text{s}^2$ angularly. (a) Initial approaching angle of 0° , DAQ time of 0.5s. (b) Initial angle of 40° , DAQ time of 0.5s. (c) Initial angle of 70° , DAQ time of 0.5s. (d) Initial angle of 0° , DAQ time of 3s.

To speed up the trail-following process, an efficient way is to increase the pace limit of translation and speed limits of both translation and rotation. In doing so, however, it also increases the likelihood of the ALL running out of the wake and getting lost. As a compromise, 5 times of pace increase, and 20 times of speed increase are made. Experiments indicate that such adjustment is adequate to remain the success rate on trail following, but the averaged tracking speed is 10 times higher. Figure 6a shows one typical tracking path. An interesting observation is that in this run, the ALL is much less hesitant locally but more zigzag globally.

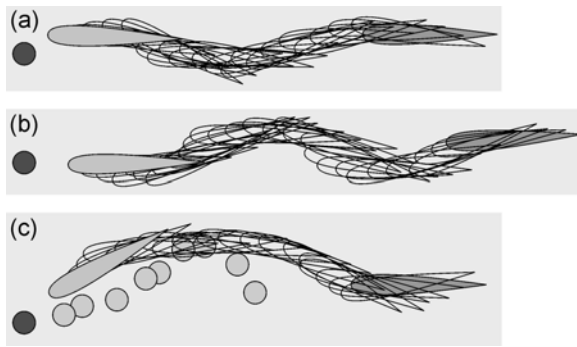


Figure 6: (a) Speeded-up step-by-step tracking path. Stepwise motion control parameters: translation and rotation ranges 5mm to 25mm and 3° to 10° , speed limits 20mm/s and $20^\circ/s$, accelerations 10mm/s^2 and $10^\circ/s^2$. (b) Continuous tracking path. Motion control parameters: pseudo stepwise translation and rotation ranges 5mm to 25mm and 3° to 10° , speed limits 2mm/s and $2^\circ/s$, accelerations 2mm/s^2 and $2^\circ/s^2$. (c) Mobile-chase-mobile tracking path. Stepwise motion control parameters are the same with (a). DAQ times for (a), (b) and (c) are all the same: 0.5s.

Another effort on speeding up is to enable real-time DAQ and decision-making during continuous running of the ALL. This way the time-consuming deceleration-stop(for DAQ)-acceleration process between two adjacent steps is eliminated. To use the same algorithm as before, DAQ and decision-making should be done during constant motion period of a current pseudo step. For this purpose, also considering the space limit of the water channel, the stepwise speed limits for both translation and rotation are set ten times lower than the run shown in Figure 6a, while the pace ranges and DAQ time remain the same. Ramp functions are used to smooth the transition from step to step. Figure 6b shows a continuous tracking path. Comparing with Figure 6a, the path is more complex globally; yet, the average tracking speed is relevant.

To further examine the developed trail-following technique, a more complicated case, mobile-chase-mobile, is explored. In this approach, the cylinder is manually moved step-by-step, sideways and upstream, while ensuring the ALL capable of discerning the wake all the time. Stepwise motion control is the same as in Figure 6a. As demonstrated in Figure 6c, the ALL eventually traps the cylinder at a corner, where the water channel restricts it from further movement.

5. FUTURE WORK

A novel bio-inspired hair-cell flow sensor has been recently developed (Chen et al, 2007; Yang et al., 2007), and construction of new ALLs utilizing arrays of such sensors is underway. Two miniature submarines equipped with newly developed ALLs, as illustrated in Figure 7, will be employed for advanced trail following study. The wake caused by a propeller-driven mini-sub (leading sub) in still water, as well as interaction of the wake with another mini-sub (following sub), will be first investigated by means of PIV. The results can serve as database for sophisticated algorithm development, which is expected to realize

mobile-chase-mobile scenario between two free-running mini-subs.

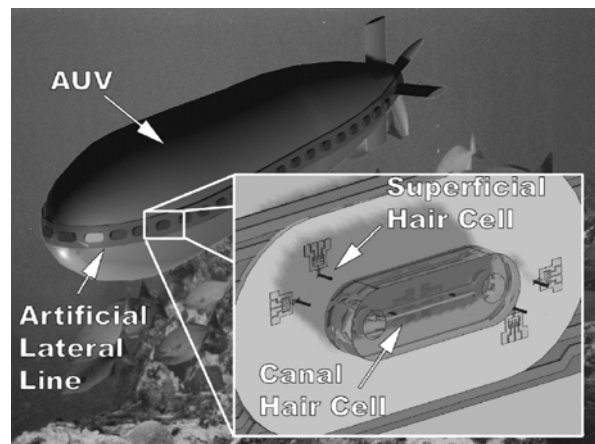


Figure 7: Composite picture showing a miniature autonomous underwater vehicle (AUV) equipped with hair-cell sensor based ALL.

6. CONCLUSIONS

We constructed a robotized artificial lateral line (ALL) by configuring multiple conventional hot-film anemometers into a fish shape on a robotic platform. Based on information collected from the ALL while it was exposed in a wake, and on decision made using specially developed algorithm, we realized autonomous trail following in various scenarios. This bio-inspired research will greatly benefit man-made underwater vehicles by giving them a third sense in addition to vision and sonar.

ACKNOWLEDGEMENTS

We gratefully thank Dr. Charlotte Barbier and Professor Joseph Humphrey at University of Virginia for their numerical simulation on a cylinder wake. This work is supported by the Bioinspired Concepts (BIC) program, funded by the Air Force Office of Scientific Research (AFOSR), and the BioSenSE program, funded by the Defense Advanced Research Projects Agency (DARPA).

REFERENCES

- Bleckmann, H., 1994, *Reception of Hydrodynamic Stimuli in Aquatic and Semiaquatic Animals*, Stuttgart, New York.
- Chen, J. and Liu, C., 2003, "Development and characterization of surface micromachined, out-of-plane hot-wire anemometer", *Journal of Microelectromechanical Systems*, Vol. 12, pp. 979-88.
- Chen, N., Tucker, C., Engel, J., Yang, Y., Pandya, S. and Liu, C., 2007, "Design and characterization of bio-inspired artificial hair cell sensor for flow sensing with ultra high velocity and angular sensitivity", *Journal of Microelectromechanical Systems*, submitted.
- Coombs, S. and Janssen, J., 1990, "Behavioral and neurophysiological assessment of lateral line sensitivity in

the mottled sculpin, *Cottus bairdi*”, *Journal of Comparative Physiology A*, Vol. 167, pp. 557-567.

Dijkgraaf, S., 1962, “The functioning and significance of the lateral-line organs”, *Biological Reviews*, Vol. 38, pp. 51-105.

Engelmann, J., Hanke, W., Mogdans, J. and Bleckmann, H., 2000, “Neurobiology - Hydrodynamic stimuli and the fish lateral line”, *Nature*, Vol. 408, pp. 51-52.

Hassan, E. S., 1986, “On the discrimination of spatial intervals by the blind cave fish (*Anoptichthys jordani*)”, *Journal of Comparative Physiology A*, Vol. 159, pp.701-710.

Liao, J. C., Beal, D. N., Lauder, G. V. and Triantafyllou, M. S., 2003, “Fish exploiting vortices decrease muscle activity”, *Science*, Vol. 302, pp. 1566-1568.

Pandya, S., Yang, Y., Jones, D.L., Engel, J. and Liu, C., 2006, “Multisensor processing algorithms for underwater dipole localization and tracking using MEMS artificial lateral line sensors”, *EURASIP Journal on Applied Signal Processing*, Vol. 2006, Article ID 76593, 8 pages.

Partridge, B. L. and Pitcher, T. J., 1980, “The sensory basis of fish schools: relative roles of lateral line and vision”, *Journal of Comparative Physiology A*, Vol. 135, pp. 315-325.

Pohlmann, K., Grasso, F. W. and Breithaupt, T., 2001, “Tracking wakes: The nocturnal predatory strategy of piscivorous catfish”, *The Proceedings of the National Academy of Sciences*, Vol. 98, pp. 7371-7374.

Yang, Y., Chen, J., Engel, J., Pandya, S., Chen, N., Tucker, C., Coombs, S., Jones, D.L. and Liu, C., 2006, “Distant touch hydrodynamic imaging with an artificial lateral line”, *The Proceedings of the National Academy of Sciences*, Vol. 103, pp. 18891-18895.

Yang, Y., Chen, N., Tucker, C., Engel, J., Pandya, S. and Liu, C., 2007, “From artificial hair cell sensor to artificial lateral line system: development and application”, *MEMS 2007 – 20th IEEE International Conference on Micro Electro Mechanical Systems*, Kobe, Japan, January 21-25, 2007.

Yang, Y., Pandya, S., Jones, D.L., Tucker, C., Chen, J., Engel, J. and Liu, C., 2007, “Recovery of rectified signals from hot-wire anemometers exposed in bidirectional flows”, *Experiments in Fluids*, submitted.